TEMs, TIE2-expressing monocytes; MELD, model for endstage liver disease

Table.3: The assessment of diagnostic value of the TEMs, AFP and PIVKA-II by ROC analyses

Discrimination between	Parameter	AUC	Cut off value	Sensitivity (%)	Specificity (%)	Positive predictive values (%)	Negative predictive values (%)
HCC and CLD	TEMs	0.85	1.46	86.1	71	76.3	82.4
	AFP	0.69	10	65.9	43.9	65.9	56.1
	PIVKA-II	0.77	47	56.3	96.5	97.8	44.5
	ANG-2	0.62	2681	51.4	67.3	52.8	64
HCC and LC	TEMs	0.93	2.75	81.3	90	89.7	81.8
	AFP	0.61	10	71.9	32.1	54.8	50
	PIVKA-II	0.79	39	64.5	93.3	95.2	56
	ANG-2	0.57	2440	68.8	52	47.8	72.2

The optimal cut-off point was determined as those yielding the minimal value for $(1–\text{sensitivity})^2$ + $(1–\text{specificity})^2$. Such point with those sensitivity and specificity values is the closest to (0, 1) point on ROC curve. .

AUC, Area under the curve; TEMs, TIE2-expressing monocytes; CLD, chronic liver disease; LC, liver cirrhosis; ANG-2, angiopoietin-2

Supplementary Table.1: The inclusion and exclusion criteria for the enrollment of patients

・ Eligible criteria for patients with hepatocellular carcinoma (HCC)
1) PS: 0～2 (ECOG PS)
2) Age: 40 - 80 years
3) Viable HCC was diagnosed by imaging analyses, such as CT and/or MRI.
Histological diagnosis is optional depending on the availability for tissue samples.
4) De novo as well as recurrent HCC are included
5) Patients who were tolerable for trans-catheter arterial chemo-embolization therapy,
local ablation therapy and/or surgical resection of the tumor
・ Eligible criteria for patients with chronic liver disease
1) PS: 0～2 (ECOG PS)
2) Age: 40 - 80 years
3) The presence of HCC was excluded by imaging analyses
4) Chronic hepatitis or liver cirrhosis was clinically diagnosed by biochemical and imaging examinations
・ Exclusion criteria for patients
1) Pregnant women
2) Patients with bleeding tendency (%prothrombin time<50%, platelet counts<30000/mm^3)
3) Patients with autoimmune hepatitis, primary biliary cirrhosis or primary sclerosing cholangititis
4) Patients with autoimmune diseases in any organs
5) Patients whom the attending doctors determined as ineligible

PS, Performance status; ECOG, Eastern Cooperative Oncology Group

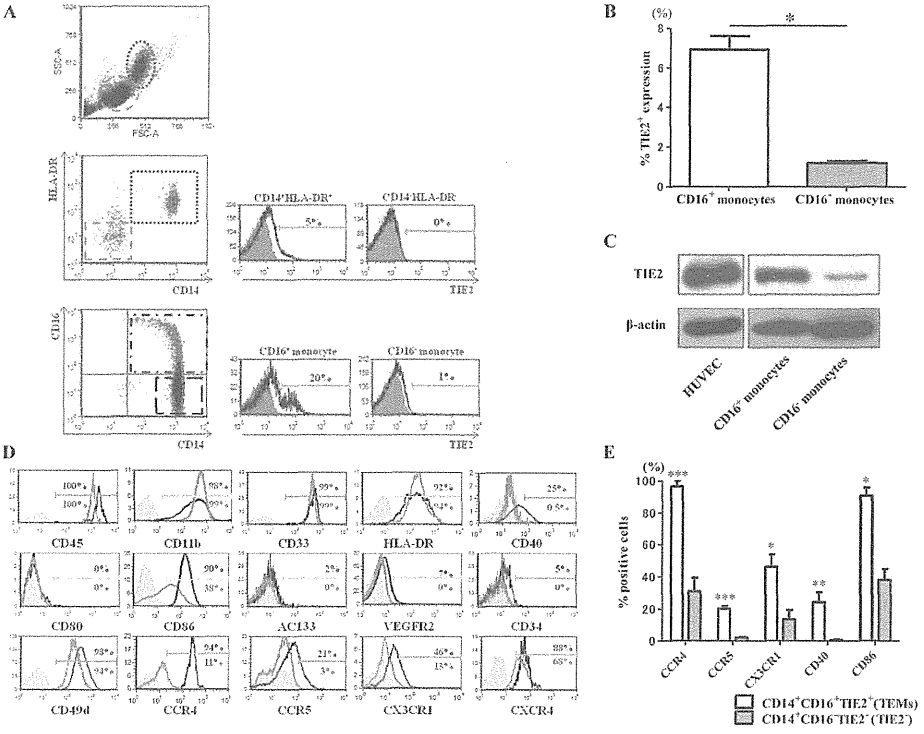

Fig. 1: Identification and phenotypic analyses of TEMs as CD14+CD16+TIE2+ cells in the peripheral blood.
A. PBMC obtained from HCC patients were stained and analyzed by flow cytometry. CD14+ monocytes were divided into two distinct subsets, CD14++CD16- and CD14+CD16+ cells. These cells were examined for TIE2 expression. The numbers in the histograms depict the percentages of gated cells. Representative plots from three patients are shown.
B. Frequencies of TIE2 in CD14+ monocytes were compared among two distinct subsets; CD16+ monocytes and CD16- monocytes, See Fig.1A. The bars indicate mean ± SE of 89 patients. *: $p<0.0001$ by Mann-Whitney nonparametric U test.
C. Western-blot analysis of TIE2 expression in FACS-sorted CD14+CD16+ and CD14++CD16- cells from HCC patients. As shown, the bands were TIE2 (140 kDa molecular weight) (the top panels) and those are β-actin (45 kDa molecular weight) (the bottom panels), respectively. The representative results of three series of experiments from 7 HCC patients are shown.
D. TEMs and TIE2- monocytes in the periphery were gated and analyzed for the expression of various molecules, as indicated in the histogram plots. The filled light gray line, black line and gray line depict the negative control, the expression of relevant markers in TEMs and TIE2- monocytes, respectively. The percentage of the marker-positive cells is shown in the histograms. The upper numbers are for TEMs and the lower ones are for TIE2- monocytes. The representative plots of six series of experiments are shown.
E. Comparative analyses of the expression of CCR4, CCR5, CX3CR1, CD40 and CD86 between TEMs and TIE2- monocytes, assessed by FACS as described above. The bars indicate mean ± SE of six series of experiments. *: $p<0.05$, **: $p<0.005$, ***: $p<0.001$ by Mann-Whitney non-parametric U test.
254x190mm (300 x 300 DPI)

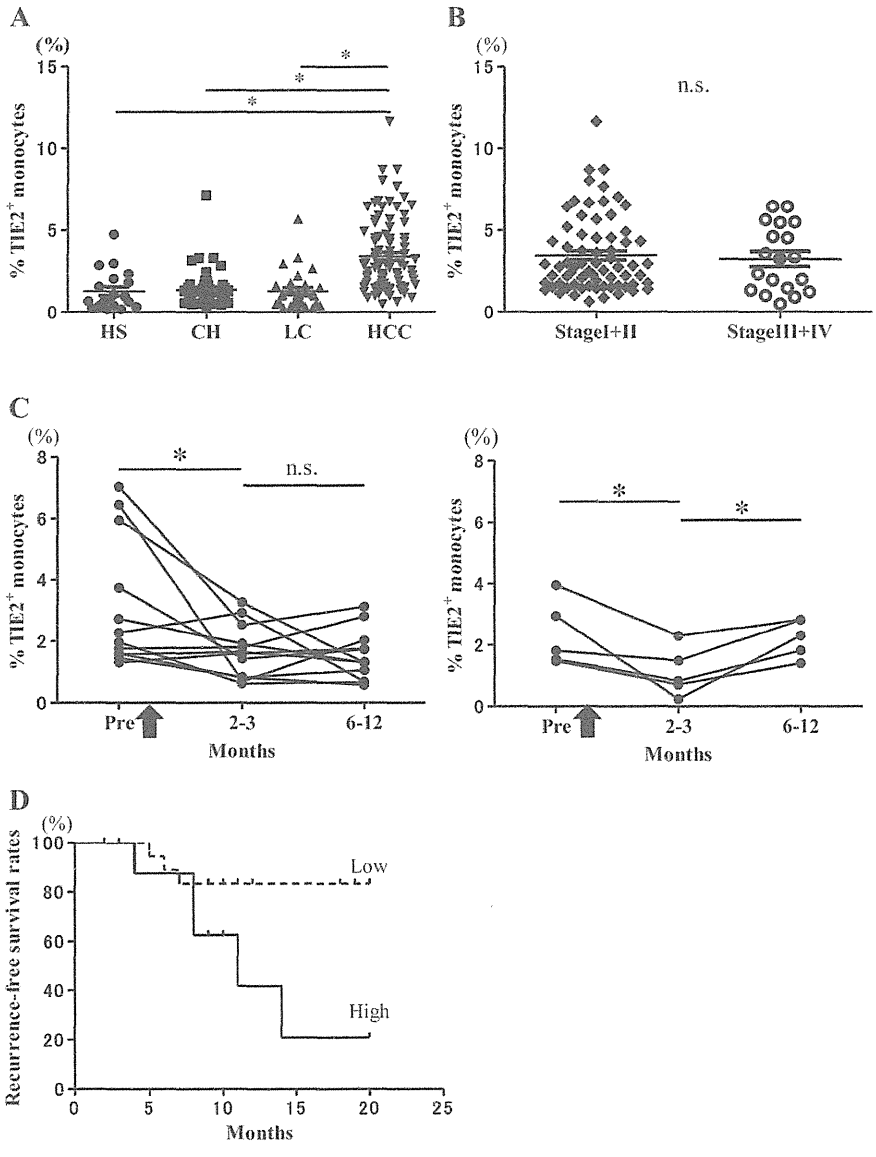

Fig. 2: Peripheral frequency of TEMs is increased in patients with HCC, with changes paralleling post therapeutic HCC recurrence.

A. Frequencies of peripheral TEMs in CD14+ monocytes are shown in four groups of HCV-positive patients; HS, CH, LC and HCC, see Table.1. *: $p<0.0001$ by Kruscal-Wallis test with Dunn's multiple comparison test.

B. Frequencies of peripheral TEMs in HCC patients at different clinical TNM stages (early stage; I+II; n=70, advanced stage; III+IV; n=19). n.s., not significant by Mann-Whitney nonparametric U test.

C. In patients who underwent RFA therapy or resection of HCC, the frequencies of TEMs in CD14+ monocytes were examined serially after confirmation of complete ablation or operation to remove HCC lesions. The bold arrows depict the time point of the RFA therapy or the operation. Both panels depict the frequencies of TEMs in patients before and after the treatment. The left panel shows the results of TEMs in patients without HCC recurrence (n=12) as assessed by CT/MRI examinations, while the right panel shows the results in patients with HCC recurrence (n=5), respectively. *: $p<0.05$ by Paired t-test.

D. In patients with HCC who underwent RFA or the operation, the recurrence-free survival rate after the

treatment was compared between those with TEMhigh (frequency of TEMs ≥ 2.75; n=45) and TEMlow (frequency of TEMs < 2.75; n=44) using the Kaplan-Meier method, with the log-rank test for comparison. TEMhigh and TEMlow , see Table 2. p = 0.047.
190x254mm (300 x 300 DPI)

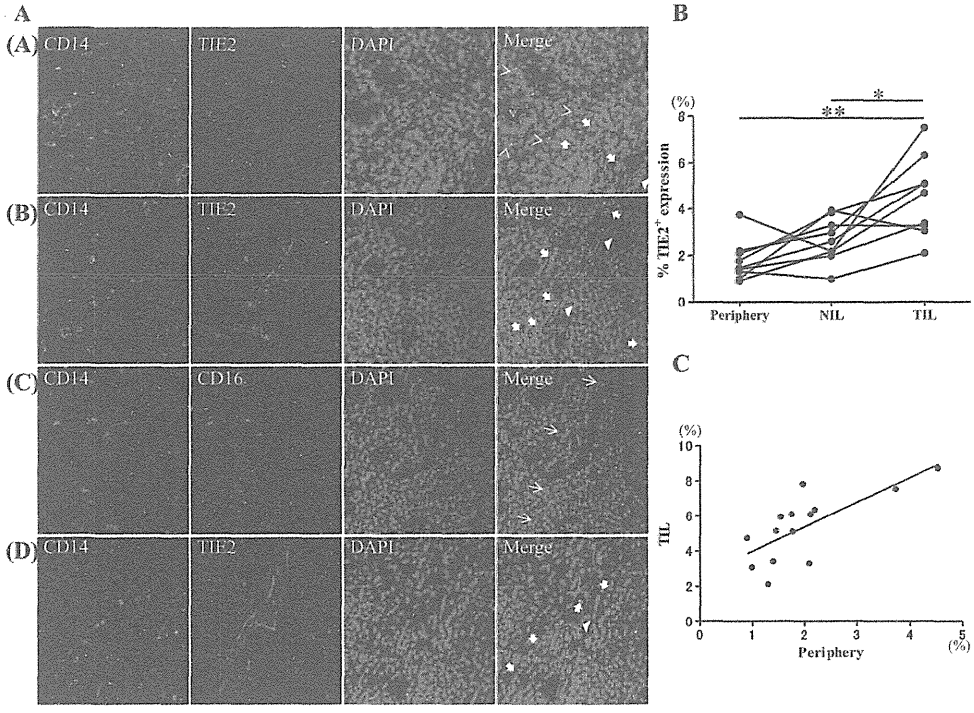

Fig. 3: TEMs are observed in perivascular areas of HCC tissue, and their frequency is higher in HCC tissue than in the periphery.

A. Immunofluorescence staining was performed as described in Materials and Methods. The staining for CD14 (green), CD16 (red) and TIE2 (red) identifies CD14+TIE2-, CD14+TIE2+, CD14+CD16- cells and CD14+CD16+ monocytes in human liver tissue (blue: nuclei counterstained with Dapi). Representative results of the resected samples obtained from 12 HCC patients are shown. The panels show CD14+TIE2+ cells (A, B, D) and CD14+CD16+ cells (C) in the perivascular area of HCC tissue (magnification, 400×), Bold arrows depict CD14+TIE2+ cells, thin arrows CD14+CD16+ cells, bold arrowheads vascular endothelial cells (TIE2+CD14-) and thin arrowheads CD14+TIE2- cells.

B. The frequencies of TEMs in 9 patients with HCC are compared for those in the peripheral blood or in the liver. Liver-infiltrating leukocytes are divided into two distinct groups: leukocytes infiltrating non-tumor tissue (NIL) and tumor-infiltrating leukocytes (TIL). These cells were stained using anti-human CD14, CD16 and TIE2 mAbs. The analyses were performed as described in Materials and Methods. The samples were obtained from nine patients who underwent tumor resection. *: $p<0.05$, **: $p<0.0005$, by Paired t-test.

C. The correlation is analyzed between the frequencies of TEMs in PBMC and those in tumor-infiltrated lymphocytes. Analysis (n=14) was based on Pearson's correlation coefficient. P = 0.003, R2 = 0.53.

254x190mm (300 x 300 DPI)

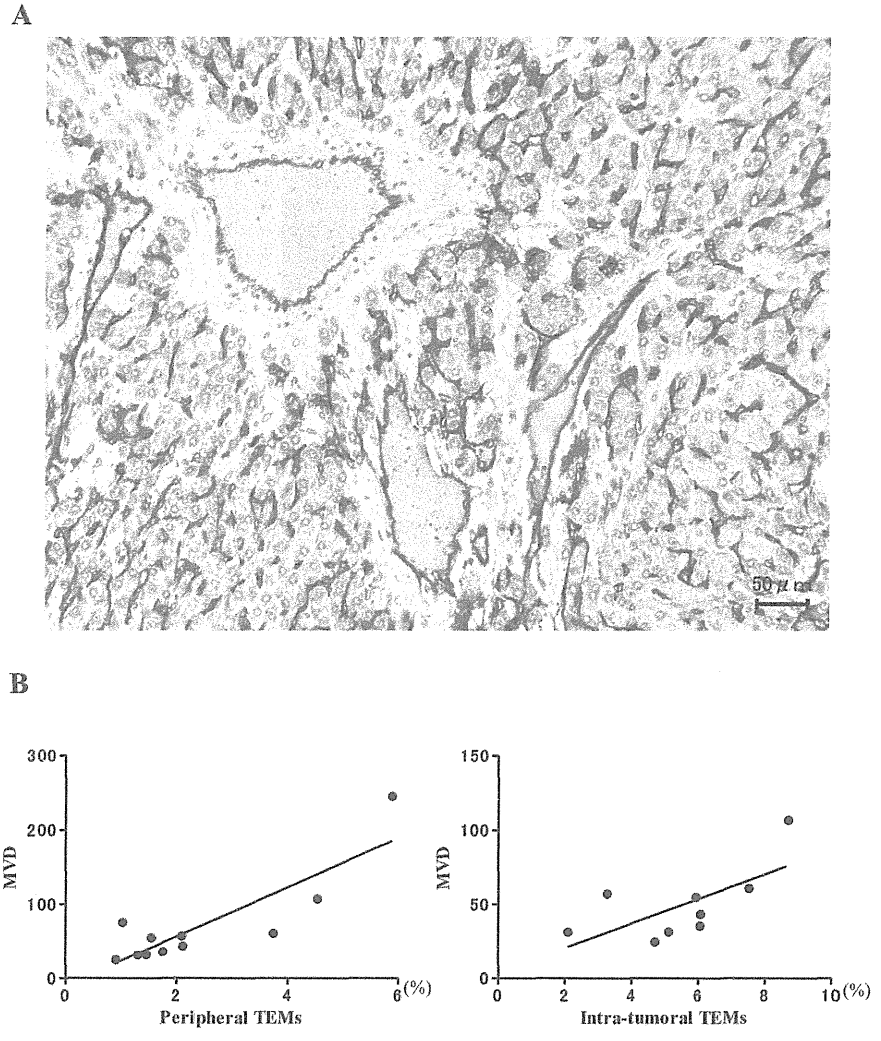

Fig. 4: The degree of microvessels in HCC is correlated with the frequency of TEMs
A. Assessment of neo-vascularization in HCC tissue was performed by staining CD34+ cells in the resected samples obtained from patients with HCC. Immunohistochemical staining for CD34 was done as described in Materials and Methods. The CD34+ cells were mainly confined to the cytoplasm of vascular endothelial cells as brownish yellow granules. Microvessels were represented by brownish yellow capillaries or small cell clusters. Representative results are shown. The panel shows a tumor cell area of a high grade.
B. The correlation is analyzed between TEM frequencies and the counts of CD34+ cells (MVD values) in relevant patients. The panels show the correlation of peripheral (left: n=11) or intra-tumoral TEM frequencies (right: n=9) and MVD ($p = 0.0009$, $R2 = 0.72$ and $p = 0.04$, $R2 = 0.44$, respectively). Analysis was based on Pearson's correlation coefficient.
190x254mm (300 x 300 DPI)

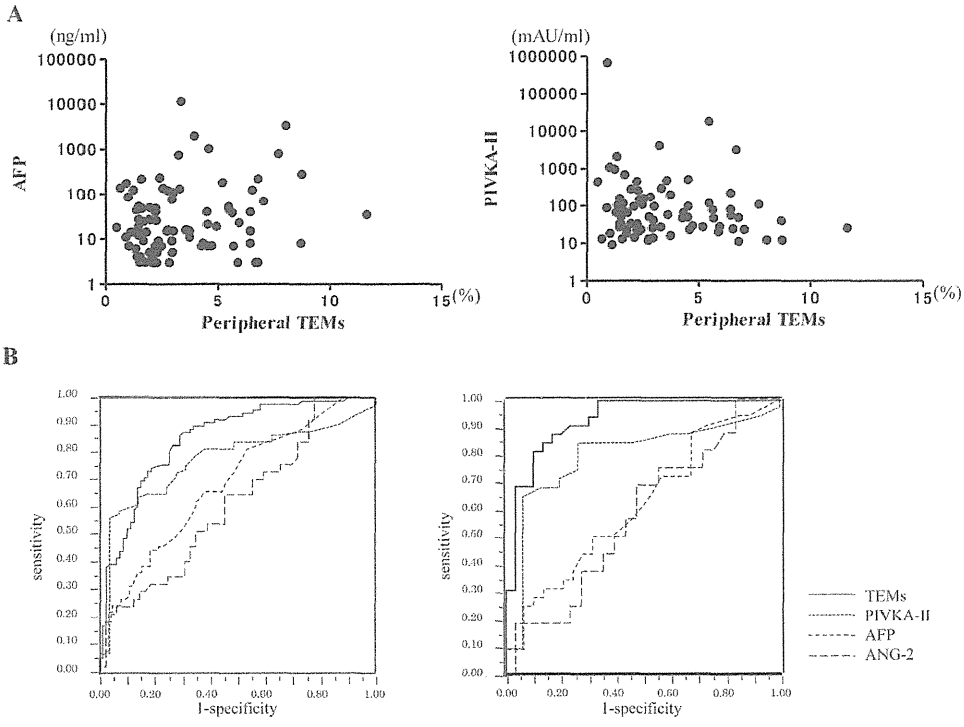

Fig. 5: Frequency of TEMs is superior as a diagnostic for HCC to common tumor markers or angiogenesis factor.

A. Correlation between TEM frequency and AFP (n=87) or PIVKA-II (n=81) was analyzed using Pearson's correlation coefficient. P = 0.45, R2 = 0.007 or P = 0.27, R2 = 0.02, respectively.

B. ROC analyses were performed in order to assess the diagnostic value of TEM frequency for differentiating HCC (n=89) from chronic liver disease (CLD, n=79) or liver cirrhosis (LC, n=30). The left panel shows the diagnostic value of TEMs, PIVKA-II, AFP and angiopoietin-2 (ANG-2) for HCC from CLD and the right panel shows those for HCC from LC, respectively.

254x190mm (300 x 300 DPI)

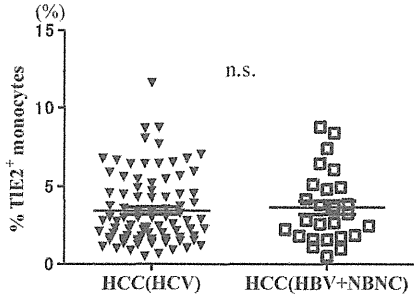

Supplementary figure 1: Frequency of TEMs is comparable in HCC patients regardless of etiology.
The frequencies of peripheral TEMs are shown for HCC patients with or without HCV infection (n=89 and n=26, respectively). The group without HCV infection included patients with HBV infection or those without HBV nor HCV (HBV-HCC and Non-B, Non-C [NBNC] HCC patients). n.s., not significant by Mann-Whitney non-parametric U test.
254x190mm (300 x 300 DPI)

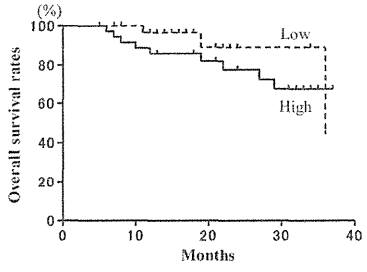

Supplementary figure 2: Peripheral frequency of TEMs is not related to the overall survival in patients with HCC.
In patients with HCC who underwent RFA or the operation, the overall survival rate after the treatment was compared between those with TEMhigh (frequency of TEMs≥2.75; n=45) and TEMlow (frequency of TEMs < 2.75; n=44) using the Kaplan-Meier method, with the log-rank test for comparison. TEMhigh and TEMlow , see Table 2. P=0.36
254x190mm (300 x 300 DPI)

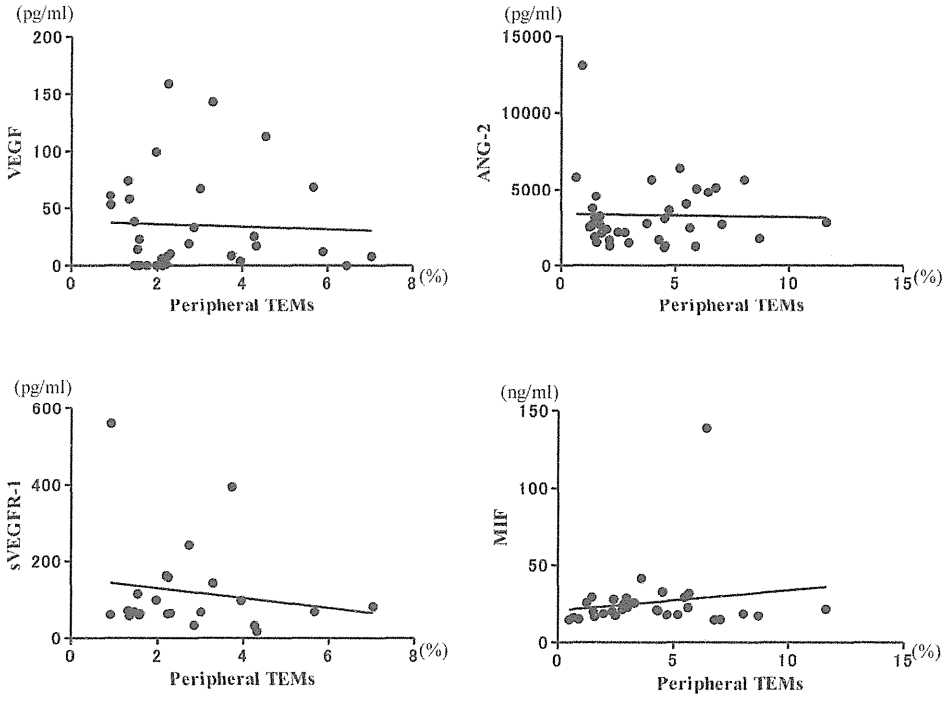

Supplementary figure 3: All plots indicate the correlation between TEM frequency and VEGF, ANG-2, sVEGFR-1 or MIF. The numbers of patients examined were 32, 37, 23 and 31, respectively. Analyses were based on Pearson's correlation coefficient.
254x190mm (300 x 300 DPI)

IJC
International Journal of Cancer

Comparative analyses of regulatory T cell subsets in patients with hepatocellular carcinoma: A crucial role of $CD25^{-}FOXP3^{-}$ T cells

Naruyasu Kakita[1], Tatsuya Kanto[1,2], Ichiyo Itose[3], Shoko Kuroda[1], Michiyo Inoue[1], Tokuhiro Matsubara[1], Koyo Higashitani[1], Masanori Miyazaki[1], Mitsuru Sakakibara[1], Naoki Hiramatsu[1], Tetsuo Takehara[1], Akinori Kasahara[4] and Norio Hayashi[3]

[1] Department of Gastroenterology and Hepatology, Osaka University Graduate School of Medicine, Suita, Japan
[2] Department of Dendritic cell Biology and Clinical Applications, Osaka University Graduate School of Medicine, Suita, Japan
[3] Kansai Rosai Hospital, Amagasaki, Japan
[4] Department of General Medicine, Osaka University Hospital, Suita, Japan

Regulatory T cells (Tregs) play pivotal role in cancer-induced immunoediting. Increment of $CD25^{high+}FOXP3^{+}$ natural Tregs has been reported in patients with hepatocellular carcinoma (HCC); however, the involvement of other type of Tregs remain elusive. We aimed to clarify whether $FOXP3^{-}$ Tregs are increased and functionally suppressive or not in patients with HCC. We enrolled 184 hepatitis C-infected patients with chronic liver diseases or HCC, 57 healthy subjects and 27 HCC patients with other etiology. Distinct Treg subsets were phenotypically identified by the expression of CD4, CD25, CD127 and forkhead/winged helix transcription factor (FOXP3). Their gene profiles, frequency and suppressor functions against T cell proliferation were compared among the subjects. To examine the molecules involving in Treg differentiation, we cultured naive $CD4^{+}$ T cells in the presence of HCC cells and dendritic cells. We determined two types of $CD4^{+}CD127^{-}$ T cells with comparable regulatory ability; one is $CD25^{high+}$ cells expressing FOXP3 ($CD25^{high+}FOXP3^{+}$ Tregs) and the other is $CD25^{-}$ cells without $FOXP3^{-}$ expression ($CD25^{-}FOXP3^{-}$ cells). The peripheral or intrahepatic frequency of $CD25^{-}FOXP3^{-}$ Tregs in HCC patients is higher than those in other groups, of which significance is more than $CD25^{high+}FOXP3^{+}$ cells. Of importance, $CD25^{-}FOXP3^{-}$ Tregs, but not $CD25^{high+}FOXP3^{+}$ cells, dynamically change in patients accompanied by the ablation or the recurrence of HCC. $CD25^{-}FOXP3^{-}$ T cells with $CD127^{-}IL\text{-}10^{+}$ phenotype are inducible *in vitro* from naive $CD4^{+}$ T cells, in which programmed cell death 1 ligand 1, immunoglobulin-like transcript 4 and human leukocyte antigen G are involved.. In conclusion, $CD25^{-}FOXP3^{-}$ Tregs with suppressive capacity are increased in patients with HCC, suggesting their distinct roles from $CD25^{+}FOXP3^{+}$ Tregs.

Hepatocellular carcinoma (HCC) is the fifth most common cancer and the third leading cause of cancer-related deaths in the world.[1] One of the most prevalent risk factors for HCC is hepatotropic viruses, such as hepatitis B (HBV) or C (HCV) virus.[2,3] In the process of HCC development, the involvement of tumor-induced immune suppression; *i.e.*, immunoediting, has been implicated. Regulatory T cells (Tregs) are unique subset of T cells, playing essential roles in the maintenance of immune homeostasis or in the protection of hosts from virulent infections and cancers.[4] Generally, the existence of two types of Tregs has been reported. One is naturally occurring $CD4^{+}CD25^{high+}$ Tregs, which are derived from the thymus and suppress auto-reactive T cells. The other is inducible or adaptive Tregs, including interleukin (IL)-10-secreting type-1 regulatory T cells (Tr1) and transforming growth factor (TGF)-β-producing Th3. These are inducible in the

Key words: HCC, regulatory T cells, FOXP3, CD25, CD127

Abbreviations: CTLA-4: cytotoxic T-lymphocyte antigen 4; DC: dendritic cell; FOXP3: forkhead/winged helix transcription factor; GITR: glucocorticoid-induced TNF receptor family-regulated gene; HBV: hepatitis B virus; HCC: hepatocellular carcinoma; HCV: hepatitis C virus; IL-T4: immunoglobulin-like transcript 4; LAG-3: lymphocyte-activation gene 3; PBMC: peripheral blood mononuclear cell; PD-1: programmed cell death 1; PD-L1: programmed cell death 1 ligand 1; RFA: radiofrequency ablation; RT-PCR: reverse transcription polymerase chain reaction; Tr1: type-1 regulatory T cells; Tregs: regulatory T cells

Additional Supporting Information may be found in the online version of this article.

Grant sponsors: Grant-In-Aid for Scientific Research from the Ministry of Education, Culture, Sports, Science and Technology of Japan, a Grant-in-Aid from the Ministry of Health, Labour and Welfare of Japan

DOI: 10.1002/ijc.27535

History: Received 23 Jul 2011; Accepted 28 Feb 2012; Online 15 Mar 2012

Correspondence to: Tatsuya Kanto, Department of Gastroenterology and Hepatology, Osaka University Graduate School of Medicine, 2-2 Yamadaoka, Suita 565-0871 Japan, Tel: +81-6-6879-3621, Fax: +81-6-6879-3629, E-mail: kantot@gh.med.osaka-u.ac.jp

Table 1. Clinical backgrounds of the patients enrolled in the study[1]

	HV	CH (C)	LC (C)	HCC (C)	HCC (B)	HCC (NBNC)
N	57	66	39	79	12	15
Gender (M/F)	35/22	44/22	23/16	44/35	8/4	9/6
Age (years)	56 ± 11	56 ± 18	61 ± 9	66 ± 11	56 ± 9	62 ± 13
ALT (IU/l)	ND	70 ± 15	44 ± 13	56 ± 17	65 ± 7	45 ± 11
Platelets ($10^4/\mu l$)	ND	15 ± 4	11 ± 4	12 ± 4	13 ± 4	12 ± 4
Total bilirubin (mg/ml)	ND	0.9 ± 0.4	1.6 ± 0.4[2]	0.9 ± 0.3	0.6 ± 0.1	0.7 ± 0.3
Alb (g/dl)	ND	3.7 ± 0.5	3.3 ± 0.4	3.1 ± 0.6[2]	3.5 ± 0.2	3.6 ± 0.3
AFP (ng/ml)[3]	ND	2-115 (15)	2-347 (16)	4-33357 (43)	7-12 (10)	10-16520 (23)
TNM stage[4] (I + II/III + IV)	–	–	–	55/24	9/3	9/6

[1]All values except for AFP are expressed as mean ± standard deviation. [2]$p < 0.05$ *vs.* CH (C) group. [3]Values are expressed as range (median).
[4]Seventh edition of International Union Against Cancer TNM staging system of HCC.
Abbreviations: HV, healthy volunteers; CH (C), LC (C), HCC (C), HCV-positive chronic hepatitis, liver cirrhosis and hepatocellular carcinoma; HCC (B), HBV-positive hepatocellular carcinoma; HCC (NBNC), non-B, non-C hepatocellular carcinoma; ALT, alanine aminotransferase; Alb, albumin; AFP, alfa-fetoprotein; ND, not determined.

periphery and are endowed with the ability to suppress antigen-specific T cells.[5] Several reports have shown that natural Tregs are increased in peripheral blood and/or tumor in patients with various types of cancer.[6] In HBV-infected HCC patients, an increase in natural Tregs and their suppressor functions against antigen-specific CTLs has been reported.[7] A correlation has been observed between natural Treg frequency and recurrence-free or overall survival of HCC patients.[8] However, it is yet to be determined if a distinct Treg subset is involved or not in the development of HCC.

The forkhead/winged helix transcription factor, FOXP3, is acknowledged as a major and specific marker of Tregs, the cellular expression of which is correlated with suppressive activities.[9] However, in the differentiation from naive T cells to effector/memory T cells, FOXP3 is transiently expressed but not sustained, suggesting that some proportion of $FOXP3^+$ T cells are not regulatory but activated ones.[10] These observations suggest that using FOXP3 as a marker of functionally regulatory cells would be limited and not suitable for adaptive Tregs. In recent studies, the expression of IL-7 receptor alpha chain (CD127) was found to be downregulated in Tregs and CD127 expression to be inversely correlated with FOXP3 expression.[11,12] Moreover, CD127-negative T cells are endowed with suppressive ability irrespective of their CD25 expression.[13] Alternatively, several studies have shown that CD127 is downregulated on $FOXP3^-$ Tr1 cells.[14,15] Due to the lack of specific or appropriate markers for identification of adaptive Tregs, it is yet to be confirmed that $FOXP3^-$ T cells are adaptive Tregs. Furthermore, little is known about the precise roles of $FOXP3^-$ regulatory cells in the development of HCC.

In this study, we focused on $FOXP3^-$ Tregs and tried to elucidate whether or not such cells are associated with the presence of HCC. To assess the feasibility of $FOXP3^-$ cells as a therapeutic target for immunological control of HCC, we tried to clarify the molecular mechanisms of its induction.

Material and Methods

Subjects

Among chronically HCV-infected patients who had been followed at Osaka University Hospital, we enrolled 184 patients who were further categorized into three groups according to the stages of liver disease: chronic hepatitis (CH), liver cirrhosis (LC) and HCC groups. The clinical stage of HCC was determined according to the TNM classification system of the International Union against Cancer (seventh edition). The study protocol was approved by the ethical committee at the Osaka University Graduate School of Medicine. At enrollment, written informed consent was obtained from all patients and volunteers. Some of HCC patients in this study received radiofrequency ablation (RFA) therapy. Indication for RFA therapy was based on therapeutic guidelines for HCC promoted by the Japan Society of Hepatology.[16] After the RFA session, the efficacy of tumor ablation or HCC recurrence thereafter was evaluated by computed tomography or magnetic resonance imaging scanning. In some of the HCC patients who underwent surgical resection, cancerous and adjacent noncancerous tissues were obtained at operation for further Treg analyses. As controls, 57 healthy subjects (HS) without history of liver diseases, 27 HCC patients with HBV infection (HBV–HCC group), those without HBV and HCV (non-B–, non-C [NBNC]–HCC group). The clinical backgrounds of the subjects are shown in Table 1.

Frequency analyses of peripheral and liver-infiltrating Tregs

Peripheral blood mononuclear cells (PBMCs) were stained with a combination of various fluorescence-labeled anti-human mouse or rat monoclonal antibodies (mAbs) as reported previously (17). The mAbs for CD4, CD25, CD127, FOXP3 and IL-10 were purchased from Becton Dickinson Biosciences (San Jose, CA). Fresh liver specimens were

washed twice with phosphate-buffered saline and were diced into 0.5 mm pieces. After these pieces were passed through a nylon mesh, liver-infiltrating lymphocytes were isolated by Ficoll-Hypaque density gradient centrifugation. These cells were stained with fluorescence-labeled Abs as performed for PBMC. For the analyses of FOXP3 and IL-10, we performed intracellular staining using a human FOXP3 staining kit (BD Biosciences) according to the manufacturer's instructions. The stained cells from PBMC or liver were analyzed by FACS Canto (BD Biosciences) and Cell Quest software.

Functional analysis of regulatory T cell subsets

To obtain live Tregs for functional analyses, we collected four populations of $CD4^+$ T cells according to the patterns of CD25 and CD127 expressions by FACS Aria (BD Biosciences). We cocultured various numbers of sorted cells with 1×10^5 allogenic naive $CD4^+CD25^-$ T cells in the presence of agonistic anti-CD3 and anti-CD28 Abs (BD Biosciences Pharmingen) on 96-well flat-bottom plates (Corning, Corning, NY) for 5 days. The proliferation of cells was assessed by incorporation of [3H]-thymidine. To clarify the suppression mechanism by Tregs, the cells were cultured with or without separation by transwell inserts (pore size 0.4 μm, Corning). Alternatively in some experiments, the cells were cultured in the presence or absence of neutralizing 10 ng/ml anti-IL-10 or anti-TGF-β Abs (R&D Systems, Mckinley, MN) or isotype IgG.

To examine regulatory cells possess suppressive function on recall antigen-specific $CD4^+$ T cell responses, we cocultured 1×10^4 each of sorted cells from some HCC patients with 1×10^5 autologous $CD4^+$ T cells in the presence or absence of 20 μg/ml of tetanus toxoid (Sigma) for 5 days, stimulated with 10 IU/ml of recombinant human IL-2 (BD Pharmingen). The proliferation of cells was assessed using WST-8 (2-(2-methoxy-4-nitrophenyl)-3-(4-nitrophenyl) -5 -(2,4-disulfophenyl)-2H-tetrazolium, monosodium salt) reagent in the Cell Counting Kit-8 (Dojindo, Japan) according to the manufacturer's instructions.

Real-time RT-PCR

To analyze gene profiles of Tregs, we collected $CD4^+CD25^{high+}CD127^-$ and $CD4^+CD25^-CD127^-$ T cells using FACS Aria. Extraction of total RNA and subsequent real-time reverse transcription polymerase chain reaction (RT-PCR) was performed as reported previously with some modifications.[17] Assays-on-demand primers and probes (Applied Biosystems, Foster City, CA) were used to quantify FOXP3, cytotoxic T-lymphocyte antigen 4 (CTLA-4), glucocorticoid-induced TNF receptor family-regulated gene (GITR), lymphocyte-activation gene 3 (LAG3), IL-21, programmed cell death 1 (PD-1) and c-masculoaponeurotic fibrosarcoma (c-Maf) expression. The expressions of molecules were given as the relative values to the calibrator samples. To standardize the amount of total RNA, we quantified β-actin mRNA from each sample as a control of internal RNA and corrected all values with this.

Induction of $CD4^+CD25^-CD127^-FOXP3^-$ T cells from PBMC

To clarify the molecular mechanisms of Treg induction, we cultured 1×10^6 naive $CD4^+CD25^-$T cells with 1×10^5 autologous monocyte-derived dendritic cells (DCs) and mitomycin C (Sigma-Aldrich, St. Louis, MO)-treated 1×10^5 HCC cell lines, Huh7 or HepG2 (AmericanType Culture Collection, Manassas, VA) on 24-well flat-bottom plates for 5 days. Monocyte-derived DCs were generated from $CD14^+$ cells as reported previously.[18] On days 2 and 4 of the coculture, recombinant human IL-2 (10 IU/ml), IL-10 (20 IU/ml) and IL-15 (20 IU/ml; BD Pharmingen) were added to the cells. On day 6, they were stimulated with phorbol 12-myristate 13 acetate (PMA; 1 ng/ml) and ionomycin (1 μmol/l) in the presence of anti-CD3 mAb (1 μg/ml) and breferdin A (1 μg/ml) (BD Pharmingen). In some experiments, we separated relevant cells by transwell inserts (pore size 0.4 μm) or added 10 μg/ml neutralizing Abs against TGF-β (R&D), HLA-DR (BD), PD-1 (R&D), programmed cell death 1 ligand 1 (PD-L1; e-Bioscience) or immunoglobulin-like transcript 4 (IL-T4) (e-Bioscience) during the culture. Subsequently, the cells were stained with Abs for CD4, CD25, CD127, FOXP3 and IL-10 and then were subjected to FACS analysis.

Knockdown of PD-L1 and HLA-G genes in HCC cell lines by siRNA

To confirm the molecules involving Treg induction, we knocked down PD-L1 and HLA-G genes in Huh7 cells by means of RNA interference. We used the small interfering RNA (siRNA) cocktail targeting human CD274 (PD-L1) or human leukocyte antigen G (HLA-G), provided by COSMO BIO (Tokyo, Japan). Transfection of siRNA to Huh7 or HepG2 cells was performed using lipofectamine RNAiMAX (Invitrogen) according to the manufacturer's instructions. To assess the efficiency of transfection, we compared the mRNA expression of target genes before and after the procedure by real time RT-PCR.

Statistical analyses

The Jonckheere-Terpstra test was used for the analysis of dose-dependent tendency. The Mann-Whitney nonparametric *U* test was used to compare differences in unpaired samples and Kruskal–Wallis nonparametric tests were used to compare differences among multiple groups, respectively. Friedman test with Bonferroni multiple comparison tests was used to compare differences in paired samples. All tests were two-tailed, and a $p < 0.05$ was considered statistically significant.

Results

$CD4^+$ T cells with distinct patterns of CD127 and FOXP3 expression were identified

According to the expression of CD25 and CD127 in $CD4^+$ T cells, we separated them into four groups: $CD25^{high+}CD127^-$, $CD25^-CD127^-$, $CD25^{high+}CD127^+$ and $CD25^-CD127^+$ cells, respectively (Fig. 1*a*). Most of the $CD4^+CD25^{high+}CD127^-$

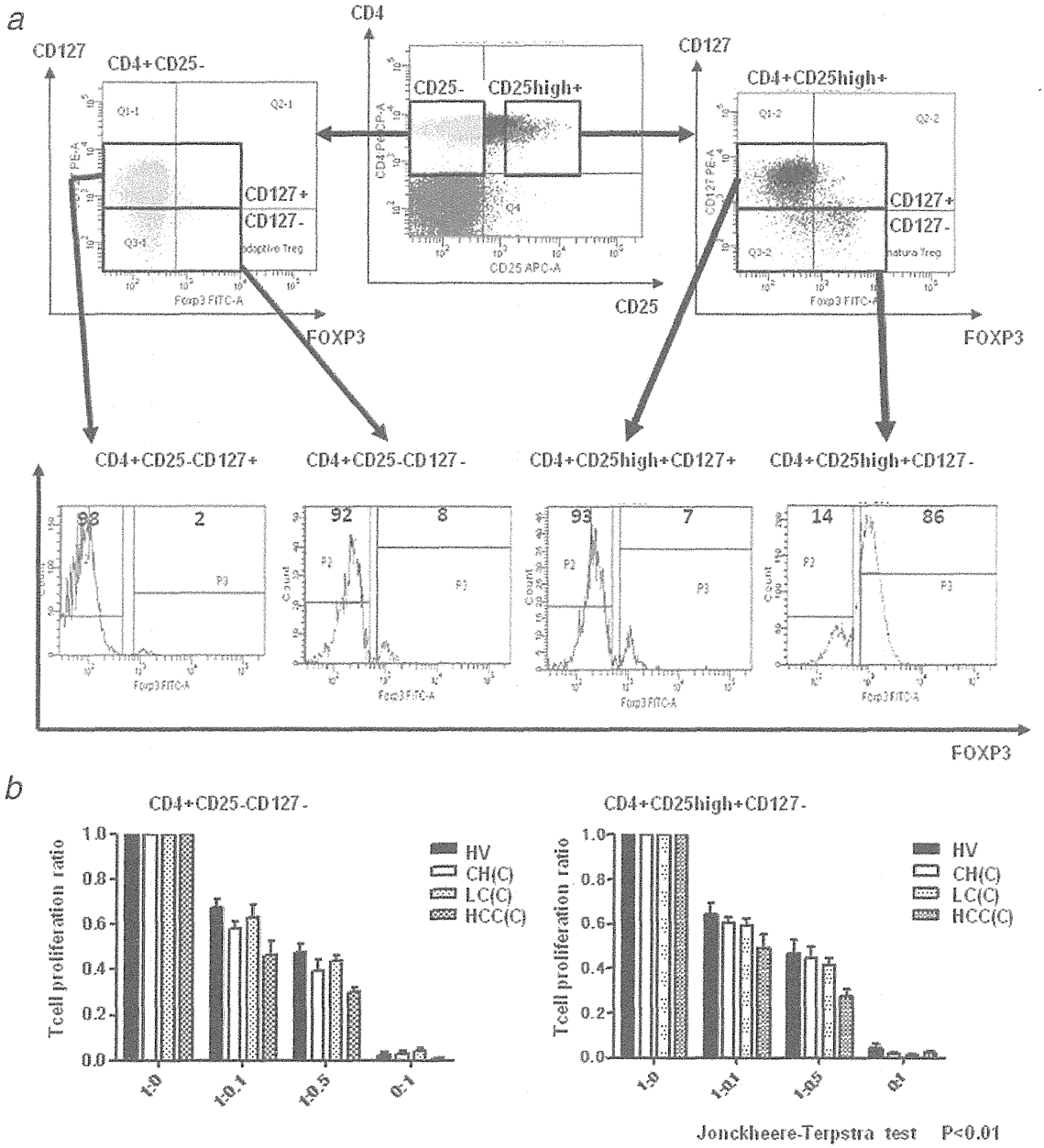

Figure 1. $CD4^+CD25^-CD127^-$ and $CD4^+CD25^{high+}CD127^-$ T cells are Tregs. (*a*) $CD4^+$ T cells are separated into four subpopulations: $CD4^+CD25^{high+}CD127^+$, $CD4^+CD25^{high+}CD127^-$, $CD4^+CD25^-CD127^+$ and $CD4^+CD25^-CD127^-$ cells, respectively. These cells were examined for FOXP3 expression. The numbers in the histograms depict the percentages of gated cells. Representative plots from three patients and donors are shown. (*b*) Sorted $CD4^+CD25^-CD127^-$ T cells and $CD4^+CD25^{high+}CD127^-$ T cells obtained from patients and healthy donors were added at various ratios to allogenic $CD4^+$ T cells stimulated with anti-CD3 and anti-CD28 Abs. After 5 days of culture, $CD4^+$ T cell proliferation was evaluated by incorporation of ^{3}H-thymidine. The bars indicate the ratio of counts per minutes (cpm) in various responders to regulatory cells ratio to those at 1:0. The results are shown as mean + SEM of ten patients or donors in each group. The dose dependency was analyzed by Jonckheere Terpstra test and comparison among the disease statuses was analyzed by Wilcoxon rank sum test with Bonferroni multiple comparison test. HV, healthy volunteers; CH(C), LC(C), HCC (C), HCV-infected chronic hepatitis, liver cirrhosis or hepatocellular carcinoma, respectively.

cells express FOXP3 (>80%). In contrast, the populations of $CD4^+CD25^-CD127^-$, $CD4^+CD25^{high+}CD127^+$ and $CD4^+CD25^-CD127^+$ lack FOXP3 expression (<10%). These results show that, except for $CD4^+CD25^{high+}CD127^-$ cells, the remaining $CD127^-$ cells lack FOXP3 and CD25 expression ($CD4^+CD25^-CD127^-FOXP3^-$).

$CD4^+CD25^{high+}CD127^-$ cells and $CD4^+CD25^-CD127^-$ T cells are suppressors against allogeneic T cells with distinct mechanisms

To examine which cell populations exert a suppressive capacity, we added each phenotype of cells separated from the subjects to allogeneic $CD4^+$ T cells. The sorted $CD4^+CD127^+$ T cells had no regulatory activities regardless of CD25 expression (data not shown). In contrast, $CD127^-$ cells, either $CD25^-$ or $CD25^{high+}$, significantly inhibited allogenic $CD4^+$ T cell proliferation in a dose-dependent manner, at comparable levels (Fig. 1*b*). Of note is that their suppressive capacity did not differ at the single cell level between patients and donors, regardless of the stage of liver disease (Fig. 1*b*). In addition, $CD127^-$ cells are anergic irrespective of CD25 expression (Fig. 1*b*). The suppressive ability of $CD4^+CD25^{high+}CD127^-$ cells was significantly abrogated by transwells and anti-TGF-β Ab, suggesting that they work in cell–cell contact-dependent and TGF-β-dependent manners (Supporting Information Fig. 1). By contrast, suppression by $CD4^+CD25^-CD127^-$ cells was alleviated by anti-IL-10 Ab but not by transwells, showing that they are contact-independent but IL-10-dependent (Supporting Information Fig. 1). These results show that $CD4^+CD25^-CD127^-$ cells possess a suppressive capacity with distinct machinery from $CD4^+CD25^{high+}CD127^-$ cells. In the setting of tetanus toxoid-reactive $CD4^+$ T cell response, each type of cells tended to be comparably suppressive (Supporting Information Fig. 2).

$CD4^+CD25^{high+}CD127^-$ and $CD4^+CD25^-CD127^-$ T cells display distinct gene profiles

$CD4^+CD25^{high+}CD127^-$ and $CD4^+CD25^-CD127^-$ T cells were sorted by FACS Aria and were subjected to real-time RT-PCR analyses. The expressions of FOXP3, CTLA-4 and GITR in $CD4^+CD25^{high+}CD127^-$ cells were higher than those in $CD4^+CD25^-CD127^-$ T cells, while those of LAG-3, IL-21, PD-1 and c-Maf in $CD4^+CD25^-CD127^-$ T cells were higher than those in $CD4^+CD25^{high+}CD127^-$ cells, respectively (Fig. 2). Thus, these two types of regulatory cells have distinct molecular profiles. As we described in the previous sections, $CD4^+CD25^-CD127^-$ cells with regulatory capacity lack FOXP3 expression (Figs. 1 and 2). Thus, we tentatively defined such cells as $CD25^-FOXP3^-$ Tregs in the following parts.

$CD25^-FOXP3^-$ Tregs are increased in HCC patients and their increments are associated with cancer progression

We compared the frequency of Treg subsets among healthy donors and HCV-infected patients. In HCC patients, $CD25^-FOXP3^-$ Tregs or $CD4^+$ $CD127^-$ $CD25^{high+}$ $FOXP3^+$ cells ($CD25^{high+}FOXP3^+$ Tregs) frequency in the periphery was significantly higher than those in other groups (Fig. 3*a*). The frequency of each type of Tregs is not correlated with HCV quantity (Supporting Information Fig. 3). These results show that the increase in $CD25^-FOXP3^-$ or $CD25^{high+}FOXP3^+$ Tregs is correlated with the development of liver cancer, but not with HCVRNA titers. Such increment of peripheral Tregs is also observed in HBV-HCC or NBNC-HCC patients (Fig. 3*a*).

Next, we compared the frequency of Tregs between PBMC and liver-infiltrating lymphocytes in HCC patients. Both $CD25^-FOXP3^-$ and $CD25^{high+}FOXP3^+$ Tregs are detected in liver-infiltrating lymphocytes, and $CD25^-FOXP3^-$ Tregs are higher in tumor-infiltrating lymphocytes than those in nontumor-infiltrating and circulating lymphocytes (Fig. 3*b*). These results demonstrate that $CD25^-FOXP3^-$ Tregs increase both in the liver and in the periphery in parallel with the development of cancer.

We serially examined the frequency of $CD25^-FOXP3^-$ Tregs and $CD25^{high+}FOXP3^+$ Tregs before and after RFA therapy. The $CD25^-FOXP3^-$ Tregs frequency dramatically decreased after successful HCC ablation and further subsided in patients without intrahepatic recurrence (Fig. 4*a*). In clear contrast, in patients with subsequent HCC recurrence, $CD25^-FOXP3^-$ Tregs increased before apparent radiological identification of HCC (Fig. 4*a*). Such dynamic frequency changes in parallel with HCC recurrence were not apparent in $CD25^{high+}FOXP3^+$ Tregs (Fig. 4*b*). Therefore, $CD25^-FOXP3^-$ Treg frequency is more closely correlated than $CD25^{high+}FOXP3^+$ Tregs with the presence or absence of HCC.

PD-L1, IL-T4 and HLA-G are involved in the induction of $CD4^+CD25^-CD127^-FOXP3^-$ IL-10^+ T cells

After the culture of naive $CD4^+$ T cells, DC and Huh7 or HepG2, we found that $CD4^+CD25^-CD127^-FOXP3^-$ cells produce IL-10 (Fig. 5*a*), whereas $CD4^+CD25^+CD127^-FOXP3^+$ cells do not (Supporting Information Fig. 4). Since $CD4^+CD25^-CD127^-$ cells use IL-10 as one of suppressor mechanisms (Supporting Information Fig. 1), such IL-10^+ $CD4^+CD25^-CD127^-FOXP3^-$ T cells are functionally competent $CD25^-FOXP3^-$ Tregs (Fig. 5*a*). In culture, the frequency of IL10^+ $CD25^-FOXP3^-$ T cells decrease in the presence of anti-TGF-β, anti-PD-1, anti-PD-L1 or anti-ILT4 Abs, with the difference being the most significant with anti-PD-L1 or anti-ILT4 Abs (Fig. 5*b*). Next, in the absence of DC or the separation of T cells from HCC cell lines significantly reduced IL10^+ $CD25^-FOXP3^-$ T cell induction, whereas separation of T cells from DC did not change it (Fig. 5*c*). These results indicate that the contact between T cells and HCC cell lines is indispensable for IL-10^+ $CD25^-FOXP3^-$ T cell induction, but the contacts between T cells and DC or between DC and HCC cell lines are not, respectively. Similarly, the addition of anti-PDL1 or anti-IL-T4 Abs to this culture resulted in suppression of IL-10^+ $CD25^-FOXP3^-$ T cell induction, regardless of the presence of transwells (Fig. 5*c*).

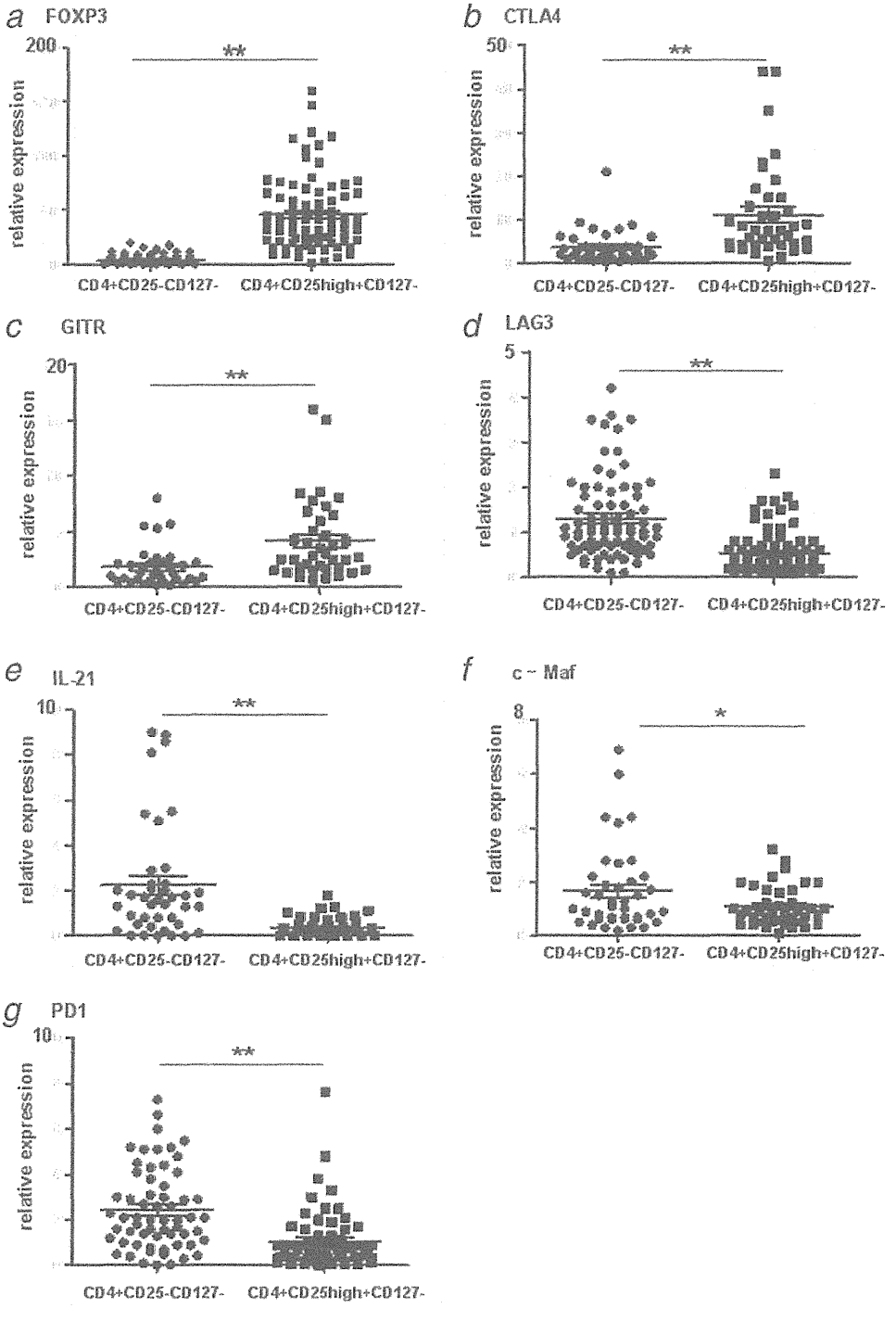

Figure 2. $CD4^+CD25^-CD127^-$ T cells and $CD4^+CD25^{high+}CD127^-$ T cells display distinct gene profiles. Sorted $CD4^+CD25^-CD127^-$ cells and $CD4^+CD25^{high+}CD127^-$ cells from PBMC of HCC patients were subjected to real-time RT-PCR for the analyses of FOXP3 (*a*), CTLA4 (*b*), GITR (*c*), LAG3 (*d*), IL-21 (*e*), c-Maf (*f*) and PD1 (*g*). The results are shown in relative expression of relevant genes to those of β-actin. *: $p < 0.05$; **: $p < 0.01$ by Mann-Whitney *U* test with Welch's correction.

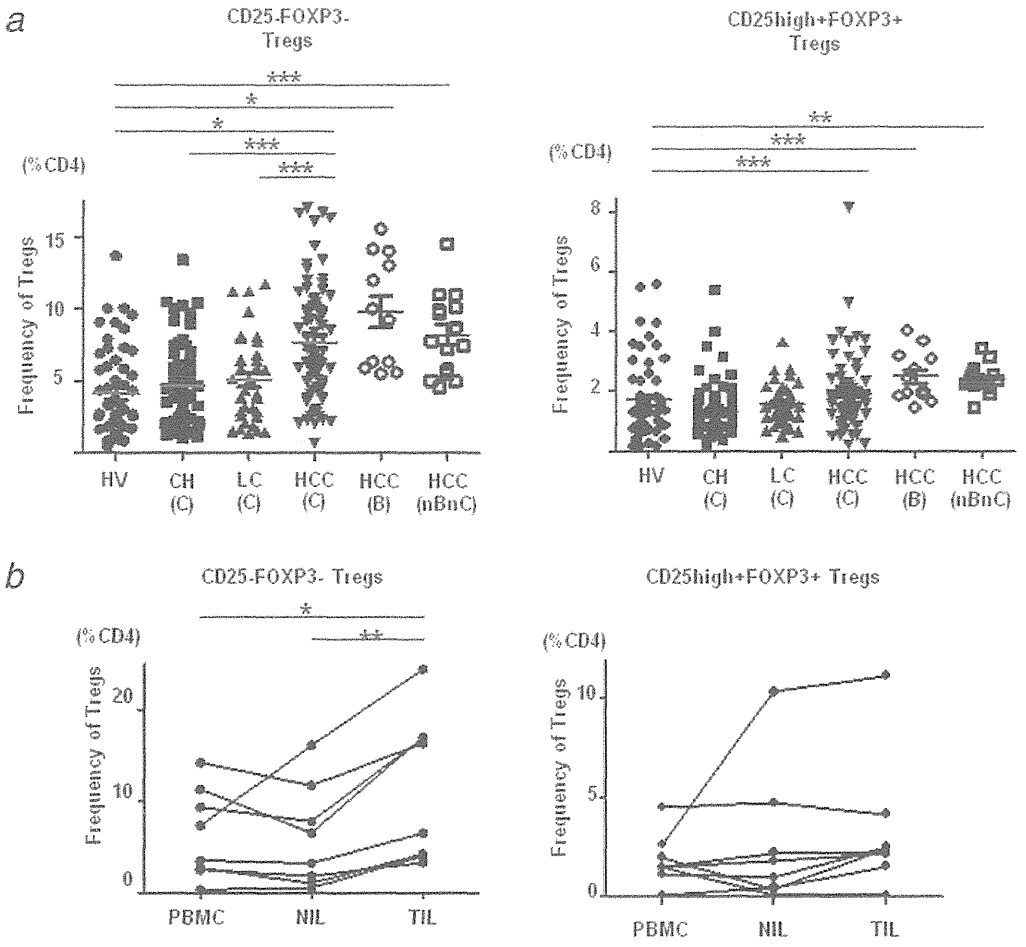

Figure 3. $CD25^{-}FOXP3^{-}$ Tregs and $CD25^{high+}FOXP3^{+}$ Tregs increase in HCC patients both in the periphery and in the liver. (*a*) The frequencies of $CD25^{-}FOXP3^{-}$ Tregs ($CD4^{+}CD25^{-}CD127^{-}$ $FOXP3^{-}$) and $CD25^{high+}FOXP3^{+}$ Tregs ($CD4^{+}CD25^{high+}CD127^{-}FOXP3^{+}$) in $CD4^{+}$ T cells were compared among the groups. HV, healthy volunteers; CH(C), LC(C), HCC (C), HCV-infected chronic hepatitis, liver cirrhosis or hepatocellular carcinoma, respectively; HCC (B), HBV-positive; HCC (nBnC), HCV-negative and HBV-negative HCC patients. The horizontal bars indicate mean ± standard deviation. *: $p < 0.05$; **: $p < 0.01$; ***: $p < 0.001$ by Kruskal–Wallis test with Dunn's multiple comparison test. (*b*) $CD25^{-}FOXP3^{-}$ Tregs and $CD25^{high+}FOXP3^{+}$ Tregs are present in tumor-infiltrating lymphocytes of HCC patients. Lymphocytes from HCC, nontumor liver tissue and PBMC were collected from identical nine HCC patients, and the frequency of $CD25^{-}FOXP3^{-}$ Tregs and $CD25^{high+}FOXP3^{+}$ Tregs in them was compared. PBMC, peripheral blood mononuclear cells; NIL, nontumor tissue infiltrating lymphocytes; TIL, tumor-infiltrating lymphocytes. *: $p < 0.05$; **: $p < 0.01$, by Friedman test with Bonferroni multiple comparison test.

IL-T4 is expressed on DC and transmits inhibitory signals after ligation with HLA-G. To confirm that the HLA-G and PD-L1 expressed in HCC are responsible for $IL10^{+}$ $CD25^{-}FOXP3^{-}$ T cell induction, we knocked down HLA-G and/or PD-L1 in Huh7 cells by siRNA and subjected them to the abovementioned *in vitro* cultures (Fig. 5*d*). As a result, $IL10^{+}$ $CD25^{-}FOXP3^{-}$ T cell frequency is significantly decreased in the presence of siRNA-treated HCC, but not with mock-transfected HCC (Fig. 5*e*). These results demonstrate that DC and HCC cells are actively involved in IL-10^{+} $CD25^{-}FOXP3^{-}$ T cell induction, in which PD-L1, IL-T4 and HLA-G are indispensible.

Discussion

In this study, we focused on $CD25^{-}FOXP3^{-}$ Tregs in HCC patients, which are distinct from $CD25^{high+}FOXP3^{+}$ natural Tregs in cellular phenotypes, genetic profiles and functional aspects. We demonstrated that; (*i*) $CD4^{+}CD127^{-}CD25^{-}$ cells (as defined as $CD25^{-}FOXP3^{-}$ cells in this study) are endowed with suppressive capacity comparably with

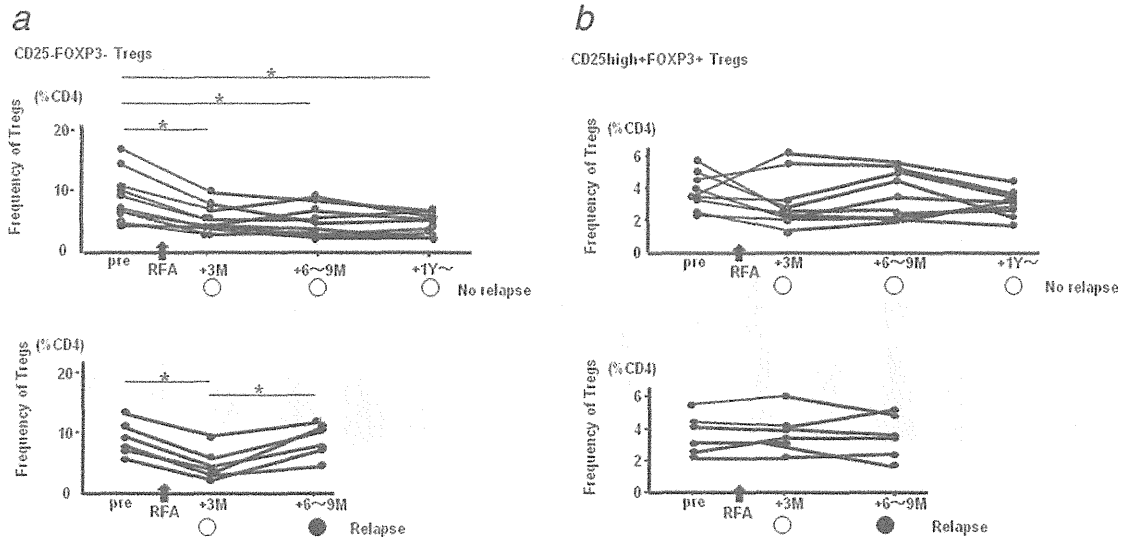

Figure 4. $CD25^{-}FOXP3^{-}$ Tregs increase in parallel with post therapeutic HCC recurrence. In HCC patients who underwent RFA therapy, frequencies of $CD25^{-}FOXP3^{-}$ Tregs (*a*) and $CD25^{high+}FOXP3^{+}$ Tregs (*b*) in $CD4^{+}$ T cells are examined serially before RFA sessions and after confirmation of complete ablation of relevant HCC lesions. Open circles (○)depict the time points without HCC recurrence under CT/MRI examinations and closed circles (●)are those with detectable HCC recurrence, respectively. Arrows indicate the time points of RFA sessions. *: $p < 0.05$ by Friedman test with Bonferroni multiple comparison test.

$CD4^{+}CD127^{-}CD25^{high+}$ cells ($CD25^{high+}FOXP3^{+}$ cells) and (*ii*) the frequency of $CD25^{-}FOXP3^{-}$ Tregs changes more dynamically than those of $CD25^{high+}FOXP3^{+}$ Tregs in correlation with post-therapeutic HCC recurrence.

Extensive studies have been carried out on the role of natural Tregs in cancer patients, of which are conventionally defined as $CD25^{high+}FOXP3^{+}$ T cells. Pharmaceutical deprivation of $CD25^{+}$ T cells *in vivo* were tried to improve immune reactivity against cancers; however, most of the study results were unsatisfactory.[19,20] Such experiences raise the possibility that the involvement of $CD25^{-}$ Tregs in the pathogenesis of certain cancers. In support for this, the existence of $CD25^{-}FOXP3^{-}$ Tregs has been reported in mice and human, in relation to viral infection or cancers.[21–23] The comparative roles of $CD25^{high+}FOXP3^{+}$ natural Tregs and $CD25^{-}$ Tregs in human diseases are still largely unknown. It is reported that CD127 expression is inversely correlated with a FOXP3 and CD127 negative population broadly encompassing regulatory cells.[11,12] Several investigators reported that CD127 expression on T cells is aberrantly regulated with regard to their functional relevance.[24,25] Taking these findings into consideration, we aimed to identify distinct type of Tregs in $CD4^{+}CD127^{-}$ population. Consequently, we found a functional regulatory subset in $CD4^{+}CD25^{-}CD127^{-}$ T cells, which differ from $CD4^{+}CD25^{high+}CD127^{-}$ Tregs in molecular profiles and inhibitory mechanisms. The profile of $CD4^{+}CD25^{-}CD127^{-}$ T cells is quite unique; they express more LAG-3, IL-21, c-Maf and PD-1 but less FOXP3, CTLA-4 and GITR than $CD4^{+}CD25^{high+}CD127^{-}$ Tregs do. In support of our results, Pot *et al.* reported that IL-27 induces IL-21 and c-Maf, which are critically involved in the differentiation of IL-10-producing Tr1.[26] As for functional aspects, we showed that $CD4^{+}CD25^{-}CD127^{-}$ cells use IL-10 as suppressive machineries, not completely but in part. Based on these characteristics, it is likely that $CD4^{+}CD25^{-}CD127^{-}FOXP3^{-}$ cells, as defined as $CD25^{-}FOXP3^{-}$ Tregs in this study, are presumed to be aforementioned Tr1 cells. Such phenotype of T cells are compatible with Tr1-like cells in human, as reported by Haringer *et al.*[14] To confirm that, several additional examinations, such as antigen-specific suppressive capacity, need to be carried out. Using tetanus toxoid as a representative of general recall antigens in this study, $CD4^{+}CD25^{-}CD127^{-}$ cells and $CD4^{+}CD25high^{+}CD127^{-}$ cells tended to be suppressive on autologous $CD4^{+}$ T cell proliferation (Supporting Information Fig. 2). Further analysis needs to be performed on this issue, using other sets of recall antigens.

To therapeutically control Tregs *in vivo*, extensive studies have been carried out to disclose the mechanisms of the induction or attraction of $FOXP3^{+}$ Tregs.[27,28] Likewise, it is tempting to consider that $CD25^{-}FOXP3^{-}$ Tregs depletion would have a favorable impact on the clinical features of the patients. Thus, identifying the molecules involved in $CD25^{-}FOXP3^{-}$, Treg induction should be carried out for the future development of Treg-oriented therapeutic approach. For this purpose, we successfully expanded $CD4^{+}CD25^{-}CD127^{-}FOXP3^{-}IL10^{+}$ cells from naive $CD4^{+}CD25^{-}$T cells. Such cultured cells contained approximately 10% of $IL\text{-}10^{+}$ cells, which subsequently

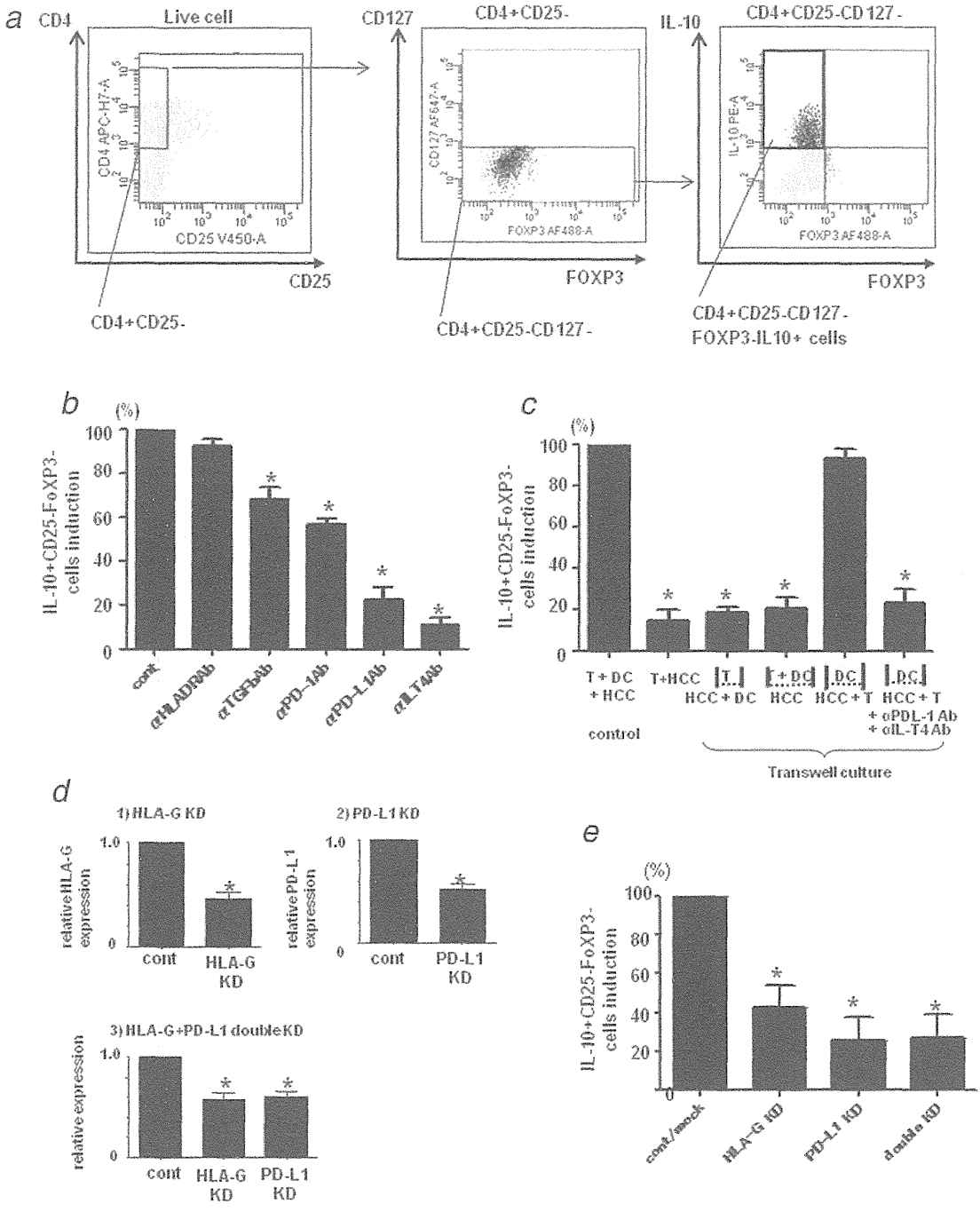

Figure 5. HLA-G and PD-L1 in HCC and IL-T4 in DC are involved in the induction of IL-10$^+$CD25$^-$FOXP3$^-$ Tregs. After culture of CD4$^+$CD45RA$^+$ naive T cells with autologous monocyte-derived dendritic cells and Huh-7 or HepG2, CD4$^+$ CD127$^-$ CD25$^-$FOXP3$^-$IL-10$^+$ T cells (IL-10$^+$CD25$^-$FOXP3$^-$ Tregs) were generated. (*a*) Representative dot plots from results of seven healthy volunteers are shown. In the abovementioned coculture system, various neutralizing/masking Abs (*b*) or transwell inserts (*c*) were added and the results were compared with the frequencies of IL-10$^+$CD25$^-$FOXP3$^-$ Tregs with or without treatments. In addition, we transfected siRNA against HLA-G and/or PD-L1 to Huh-7 and cocultured them with naive CD4$^+$ T cells and DC as the same as above. The efficiency of gene silencing was evaluated by the comparison of transcripts of HLA-G or PD-L1 with or without siRNA transfection (*d*). The frequency of IL-10$^+$CD25$^-$FOXP3$^-$ Tregs after the culture was compared with mock-transfected ones (*e*). In Figures 5-B, 5-C and 5-E, the bars indicate the ratio of IL-10$^+$CD25$^-$FOXP3$^-$ Tregs frequency (mean + standard deviation) between those with treatment and without from three series of experiments. *: $p < 0.05$ by Wilcoxon rank sum test.